International Journal of Rock Mechanics & Mining Sciences 75 (2015) 15–22

Contents lists available at ScienceDirect

International Journal of Rock Mechanics & Mining Sciences

journal homepage: www.elsevier.com/locate/ijrmms

Relationship between joint roughness coefficient and fractal dimension of rock fracture surfaces

Yanrong Li [a,b,*], Runqiu Huang [c]

[a] Taiyuan University of Technology, Taiyuan, China
[b] AGECON Ltd., Hong Kong, China
[c] State Key Laboratory of Geohazard Prevention and Geoenvironment Protection, Chengdu University of Technology, Chengdu, China

ARTICLE INFO

Article history:
Received 21 September 2014
Received in revised form
9 November 2014
Accepted 12 January 2015
Available online 7 February 2015

Keywords:
Rock joint roughness coefficient (*JRC*)
Fractal dimension
Compass-walking
Box-counting
The *h*–*L* method

ABSTRACT

Numerous empirical equations have been proposed to estimate the joint roughness coefficient (*JRC*) of a rock fracture based on its fractal dimension (*D*). A detailed review is made on these various methods, along with a discussion about their usability and limitations. It is found that great variation exists among the previously proposed equations. This is partially because of the limited number of data points used to derive these equations, and partially because of the inconsistency in the methods for determining *D*. The 10 standard profiles on which most previous equations are based are probably too few for deriving a reliable correlation. Different methods may give different values of *D* for a given profile. The *h*–*L* method is updated in this study to avoid subjectivity involved in identifying the high-order asperities. The compass-walking, box-counting and the updated *h*–*L* method are employed to examine a larger population of 112 rock joint profiles. Based on these results, a new set of empirical equations are proposed, which indicate that the fractal dimension estimated from compass-walking and the updated *h*–*L* method closely relate to *JRC*, whereas the values estimated from box-counting do not relate as closely.

1. Introduction

Discontinuities play an important role in the deformation behavior of a rock mass. Properties of the rock discontinuities include extent, orientation, roughness, infilling and joint wall strength. Roughness, which refers to the local departures from planarity, influences the friction angle, dilatancy and peak shear strength. A milestone was made by Barton [1], who puts forward an empirical equation to estimate the peak shear strength of a rock joint $\tau = \sigma \tan[JRC \log(JCS/\sigma) + \varphi_b]$, where τ is the peak shear strength of the rock joint, σ is the normal stress, *JRC* is the joint roughness coefficient, *JCS* is the strength of joint wall, and φ_b is the basic friction angle. The *JRC* of a particular rock joint profile is most often estimated by visibly comparing it to the 10 standard profiles with *JRC* values ranging from 0 to 20 [2]. This approach was also adopted by the ISRM commission on test methods in 1981 [3]. However, the visual comparison is subjective, since the user has to judge which profile his joint fits the best.

The development of objective methods was gradually advanced by researchers considering statistical parameters and the fractal dimension of the rock joint profiles [4–8]. A detailed review was carried out more recently [9] on the determination of *JRC* using statistical parameters, where empirical equations with R_z (maximum height of the profile), λ (ultimate slope of the profile) and δ (profile elongation index) were proposed and highly recommended for engineering practice as they have high correlation coefficients and are easy to calculate.

The fractal dimension (*D*) describes the degree of variation in a curve, a surface or a volume from a line, a plane or a cube. Since the work of Turk et al. [10] and Carr and Warriner [11], the fractal dimension was thought to be a suitable parameter for quantifying the roughness of a natural rock joint profile [12–18], as the fractal dimension has a minimum value of 1 for a perfectly smooth profile and a maximum value of less than 2 for an extremely rough undulating profile [19,20]. Numerous empirical equations were put forward for estimating *JRC* using *D*. However, difficulties arise when ranking the suitability of these equations and choosing a particular one to use in engineering practice, as the *D* determination methods, examined profiles and data processing methods on which the empirical equations were based are diverse.

The present study aims to review the determination of *JRC* using *D*. The definition and calculation of *D* determination methods are clearly described, followed by a detailed review of the empirical equations in the literature. The authors will repeat what the previous researchers have done to evaluate the accuracy and limitations of these equations. Finally, 112 joint profiles are utilized

* Corresponding author.
E-mail address: li.dennis@hotmail.com (Y. Li).

http://dx.doi.org/10.1016/j.ijrmms.2015.01.007

to correct and update the empirical equations for them to be better used in rock engineering.

2. Fractal dimension and its determination

To date, the fractal dimension of a rock joint profile was generally determined by compass-walking [7], box-counting [24] and the *h–L* methods [25] in rock engineering. A review of these methods is given in the following subsections in terms of definition and calculation.

2.1. Compass-walking method

The compass-walking is also called divider, a yardstick or stick-measuring method [7,21,22], and the main concept of this method is to measure a curve by "walking a compass of radius *r*" along the curve (Fig. 1). The detailed process of measurement is as follows (Fig. 1): set a compass to a prescribed radius *r*, and walk the compass along the profile, each new step starting where the previous step leaves off. For each compass of a certain radius *r*, one would get an *N* (the number of steps) for fully measuring the curve. With compasses of different radii, a set of *N*s would be obtained. If the base 10 log of the *N* values are plotted against the base 10 log of the corresponding *r* values, the slope of this plot is $-D$ [23]:

$$-D=\Delta \log N/\Delta \log r \tag{1}$$

where $\Delta \log N$ is the increment of $\log N$, and $\Delta \log r$ is the increment of $\log r$.

An alternative to the above calculation was used by Maerz et al. [7]. They counted the number *N* of dividers of length *r* needed to cover the profile and repeated this measurements for various lengths of *r*. The fractal dimension *D* is calculated in practice by plotting *Nr* versus *r* in a log–log space and equating the slope to $1-D$:

$$1-D=\Delta \log(Nr)/\Delta \log r \tag{2}$$

where $\Delta\log(Nr)$ is the increment of $\log(Nr)$ in the plot.

A modification of the traditional calculation (1) was made by Bae et al. [21]. The fractal dimension of a joint profile is defined by three parameters including *N*, *r*, and *f*, where, *N* is the number of steps for walking through a joint profile by a divider with a span of *r* (Fig. 1). The length of the joint profile was defined as $Nr+f$, where, the value *f* is obtained by measuring the remaining length shorter than *r* after excluding the length of *Nr* for the total joint profile length. The fractal dimension *D*, thus, is defined as the slope of $\log(N+f/r)$ versus $\log(r)$ according to:

$$-D=\Delta \log\,[N+(f/r)]/\Delta \log r \tag{3}$$

2.2. Box-counting method

The box-counting dimension is also known as the Minkowski–Bouligand dimension, which works as a way of determining the fractal dimension of a set in a Euclidean space, or more generally in a metric space (*X*, *d*) [24].

To calculate the fractal dimension, the joint profile is placed on an evenly-spaced grid, and the number of boxes required to fully cover the profile is counted. Suppose that *G* is the number of boxes of side length ε required to cover the profile. In practice the box-counting dimension is calculated by seeing how this number changes as the grid gets finer and is obtained by plotting *G*s against the corresponding εs in a log–log space. The slope of this plot is regarded as $-D$:

$$-D=\Delta \log G/\Delta \log \varepsilon \tag{4}$$

2.3. The h–L method

This method was firstly proposed by Xie and Pariseau [25], and was defined as:

$$D=\frac{\log 4}{\log\{2(1+\cos[\arctan(2h/L)])\}}$$
$$h=\frac{1}{M}\sum_{i=1}^{M}h_i,\quad L=\frac{1}{M}\sum_{i=1}^{M}L_i \tag{5}$$

where *L* and *h* are the average base length and the average height of "high-order" asperities of a joint, respectively (Fig. 2). A similar definition was also given in the following expression by Askari and Ahmadi [26]:

$$D=\frac{\log 4}{\log\{4\cos[\arctan(2h/L)]\}} \tag{6}$$

The difficulties in using the above two equations are the identification of the so-called "high-order" asperities of a profile and the manual measurement of their base length and height (Fig. 2). The subjectivity involved in identifying the asperities may introduce bias into the estimated *D*.

3. Review of available empirical equations

Since Turk et al. [10], who put forward the first correlation between *JRC* and *D* of a joint profile, studies of this relationship have attracted attention from researchers. Table 1 lists the empirical equations from the literature for estimating *JRC* from *D*; in the text, these equations will be referred to as T1, T2, etc., to avoid confusion with the previous six displayed and numbered equations. It is found that diverse measuring methods for determining *D* were employed, including the compass-walking, box-counting and *h–L* method. Most of the empirical equations (T1, T2, T5, T6, T7, T9, T10, T12, T13 and T17) were derived from the 10 standard *JRC* profiles proposed by Barton and Choubey [2]. Equations (T14-T16) were derived from 10 profiles published by Xu et al. [22]. Equation (T3) was derived from seven profiles published by Qin et al. [27]. Equation (T11) was derived from 42 profiles published by Jia [28]. No clear description of the data source was given for the rest of the equations. The correlation coefficients (if provided) are generally greater than 0.9, showing a close correlation between *JRC* and *D*. Most equations are not accompanied by the sampling interval and the sampling intervals (if provided) are variable.

Equations (T1–T5) take *D* as the independent variable. One of the apparent disadvantages of these equations is that they result in a *JRC* value not equal to 0 for a perfectly smooth plane. That is, they are not applicable for planar or sub-planar joint profiles.

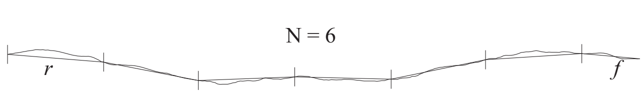

Fig. 1. Schematic of the compass-walking method for determination of *D* of a profile.

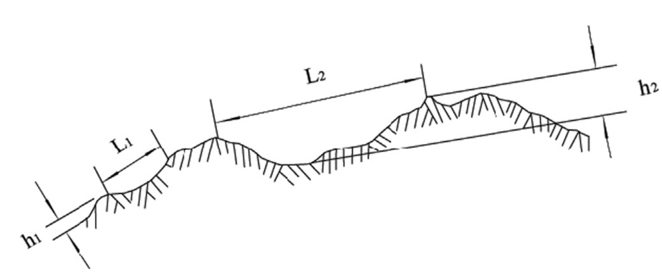

Fig. 2. Measurement of *h* and *L* in Eqs. (5) and (6) (Xie and Pariseau [25]).

Table 1
Literature review of empirical equations for estimating *JRC* by using *D*.

No.	Equation	Method	*R*	*SI*	JRC^0	*D* Range#	St. Profiles	Reference
T1	$JRC=-1138.6+1141.6D$	C-W*	–	–	3	1.0–1.0149	Y	Turk et al. [10]
T2	$JRC=-1022.55+1023.92D$	C-W*	0.9800	–	1.3700	1.0–1.0182	Y	Carr and Warriner cr
T3	$JRC=209.7517D-204.1486$	C-W	0.9470	0.5	5.6031	1.0–1.0686	N	Qin et al. [277]
T4	$JRC=172.206D-167.2946$	C-W	0.9976	–	4.9114	1.0–1.0876	Y	Zhou and Xiong [29]
T5	$JRC=7811778.928D^3-23723041.6842D^2+24014672.3562D-8103409.7809$	C-W#	0.9930	0.05	−0.1809	1.0–1.0144	Y	Bae et al. [21]
T6	$JRC=1000(D-1)$	C-W*	–	–	0	1.0–1.0200	Y	Carr and Warriner [11]
T7	$JRC=1870(D-1)$	C-W^{MR}	–	0.684	0	1.0–1.0107	Y	Maerz and Franklin [30]
T8	$JRC=1647(D-1)$	C-W	0.9600	–	0	1.0–1.0121	N	Liu [31]
T9	$JRC=1195.38(D-1)$	C-W	–	–	0	1.0–1.0167	Y	Lamas [32]
T10	$JRC=479.396(D-1)^{1.0566}$	C-W	–	–	0	1.0–1.0495	Y	Zhou and Xiong [29]
T11	$JRC=29.35(D-1)^{0.46}$	C-W	0.9045	0.02	0	1.0–1.4343	N	Jia et al. [28]
T12	$JRC=150.5335(D-1)^{0.5}$	C-W	–	–	0	1.0–1.0177	Y	Wakabayashi and Fukushige [33]
T13	$JRC=-0.87804+27.7844(D-1)/0.015–16.9304[(D-1)/0.15]^2$	C-W	0.9500	1	−0.8780	1.0005–1.0113	Y	Lee et al. [23]
T14	$JRC = 28.5 - \frac{33.18}{1+150(D-1)}$	C-W	0.9985	0.5	−4.6800	1.0011–1.0194	N	Xu et al. [22]
T15	$JRC = 100(D - 1)^{0.4}(1-\frac{1}{\exp[300(D - 1)]})$	C-W	–	0.5	0	1.0–1.0181	N	Xu et al. [22]
T16	$JRC = \frac{60(D - 1)^{1.2}}{0.006 + (D - 1)}$	C-W	–	0.5	0	1.0–1.0177	N	
T17	$JRC=15179W_d(D-1)^{1.46}$	B-C	–	–	0	–	Y	Chen [35]
T18	$JRC=53.7031(D-1)^{0.3642}$	$h–L^1$	0.9850	–	0	1.0–1.0664	N	Askari and Ahmadi [26]
T19	$JRC=85.2671(D-1)^{0.5679}$	$h–L^2$	–	–	0	1.0–1.0778	Y	Xie and Pariseau [25]

Note: SI: Sample interval; *R*: correlation coefficient; JRC^0: estimated *JRC* value for a truly smooth plane; *D* Range#: applicable range of independent value; and St. profiles: the 10 standard profiles.
C-W: Compass walking, $D=-\Delta\log N/\Delta\log r$; C-W#: Compass walking, $D=-\Delta\log[N+(f/r)]/\Delta\log r$; C-W^{MR}: Compass walking, $D=1-\Delta\log(Nr)/\Delta\log r$; B-C: Box counting, $-\Delta\log G/\Delta\log\varepsilon$; $h–L^1$: $D = \frac{\log 4}{\log\{4\cos[\arctan(2h/L)]\}}$; $h–L^2$: $D = \frac{\log 4}{\log\{2(1+\cos[\arctan(2h/L)])\}}$.
W_d : Waviness degree, equals to r/L, r the asperity height and L the projected length of the profile.

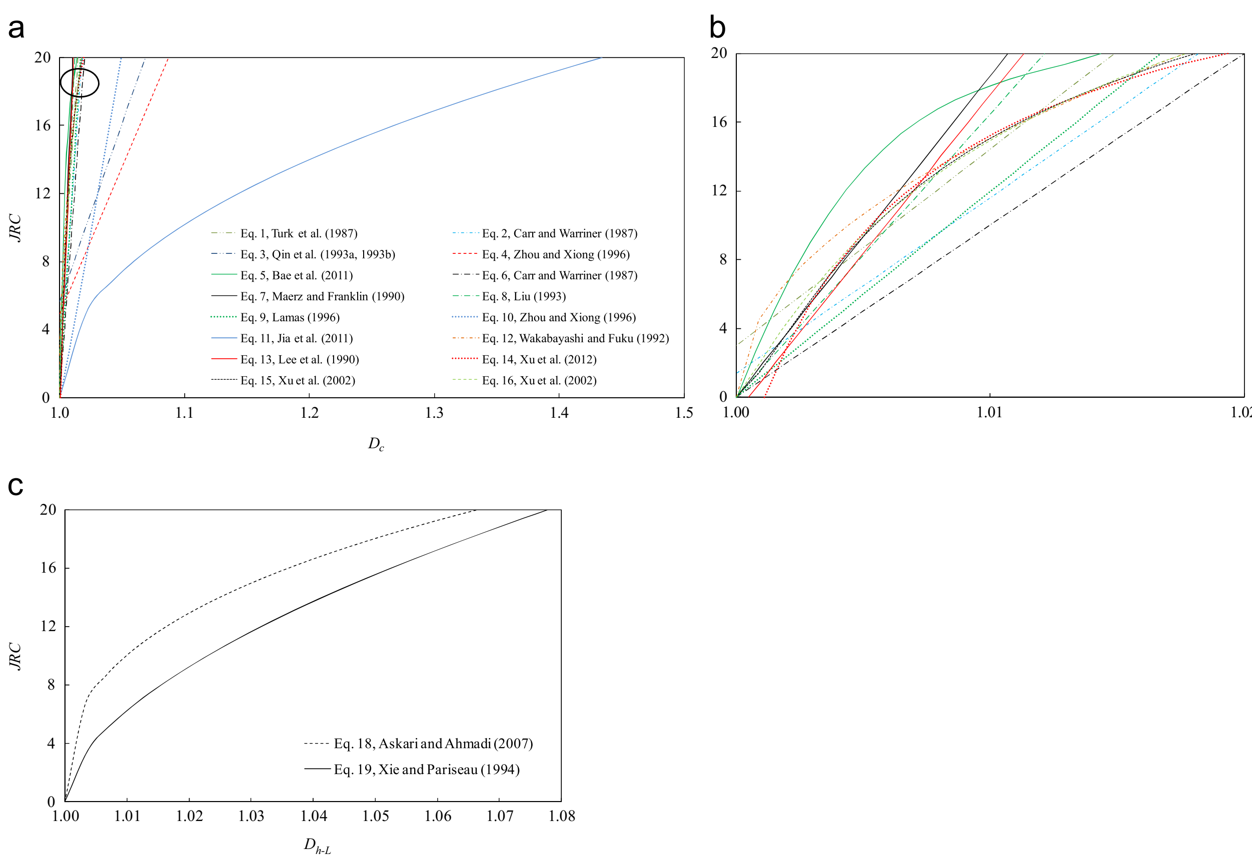

Fig. 3. Empirical relationships in literature for estimating *JRC* by means of the fractal dimension: (a) compass-walking method; (b) enlargement of the circled part in (a); (c) *h*–*L* methods. (Equations refer to Table 1).

Equations (T6–T19) take $D-1$ as the independent variable, and they are capable of evaluating a smooth joint profile.

The equations in Table 1 are plotted in Fig. 3, where Fig. 3a is for compass-walking and Fig. 3c for the *h*–*L* method. The circled part of Fig. 3a is magnified and shown to its right as Fig. 3b. Though the consistent trend shows that *JRC* increases with *D*, inconsistency does exist. Equations (T3, T4, T10 and T11) are separate from the others, to a great extent (Fig. 3a). The fractal dimensions for the densely clustered equations (the circled part) range from 1.0 to 1.02, which is much narrower than that for equations (T3, T4, T10 and T11). Correlations between *JRC* and D_{h-L} (Fig. 3c) are totally different from those with D_c (Fig. 3a and b) in terms of range of fractal dimension. The cluster (circled part) in Fig. 3a, if magnified (Fig. 3b), still shows obvious differences. This may lead to non-ignorable uncertainties when estimating *JRC*. The differences among the published equations suggest that the same *D* determination method as that used to originally develop the empirical equation must be employed when using a certain empirical equation for estimating *JRC*.

The determination method of *D* is one of the reasons leading to the inconsistency among Fig. 3a, b and c. The compass-walking method generally produces $D_c < 1.02$ for the profiles in the literature [10,23,36,37]. The *h–L* method may give a greater D_{h-L}. This is because that D_{h-L} is governed only by the "high-order" asperities of the profile (Fig. 2), while D_c is taking the average roughness level of all asperities (small and large ones).

Another reason for the inconsistency among the equations in Fig. 3 is the data source. The equations were generally based on two categories of rock joint profiles: the 10 standard profiles and those measured by the authors. In general, equations based on the 10 standard profiles show a good agreement (see the clustered part of Fig. 1a). The *JRC* values of the 42 profiles used by Jia [28] to derive equation (T11) were from visual comparison with Barton's 10 standard profiles [1], which would lead to errors in *JRC* values due to subjectivity during the comparison process. Eq. (T3) was based on seven profiles (rather than the 10 standard profiles), whose *JRC* values were determined by using Tse and Cruden's equation $JRC = -4.41 + 64.46\ Z_2$ (where Z_2 is the root mean square of the first deviation of the profile). The errors involved in this transformation might be another source of error in the *JRC* values.

After a careful verification, the authors found that the *JRC* value for each standard profile was inconsistently assigned in the literature for deriving empirical equations in Table 1 and Fig. 1. As shown in Table 2, Lee et al. [23], Bae et al. [21], Xie and Pariseau [25], Xu et al. [34] and Chen [35] took the intermediate odd numbers (i.e., 1, 3, 5, etc.) as the *JRC* value of the standard profiles, while other researchers used the values from Barton and Choubey [2]. This would certainly lead to deviation not only in the plots but also in the empirical equations derived.

The above observation and discussion suggest that the following causes are responsible for the variation of empirical equations in the literature: the origin of joint profiles, *D* determination methods and *JRC* determination methods. This study employs the compass-walking, box-counting and *h–L* methods to examine 112 joint profiles. The *JRC* values of these profiles were directly determined by back calculation of the direct shear test of rock joints with the Barton–Bandis shear strength model. Comparisons between different *D* determination methods are made together with the discussion about applicability and usability of the proposed equations.

Table 2
JRC values used in literature for deriving empirical equations in Table 1

Standard JRC profiles	1	2	3	4	5	6	7	8	9	10
JRC values recommended by Barton and ISRM	0–2	2–4	4–6	6–8	8–10	10–12	12–14	14–16	16–18	18–20
Bae et al. [21]; Xie and Pariseau [25]; Lee et al. [23]; Xu et al. [34]; and Chen [35]	1	3	5	7	9	11	13	15	17	19
Seidel and Haberfield [37]; Turk et al. [10] and this study	0.4	2.8	5.8	6.7	9.5	10.8	12.8	14.5	16.7	18.7

Divider length *r* or box side length ε (mm)	Number of dividers and the remains, $N+f/r$	Number of counted boxes, *G*
50.0	2.000	2
25.0	4.001	4
12.5	8.010	8
6.250	16.035	16
3.125	32.117	32
1.563	64.678	65
0.781	129.986	149
0.391	261.217	304
0.200	511.121	603

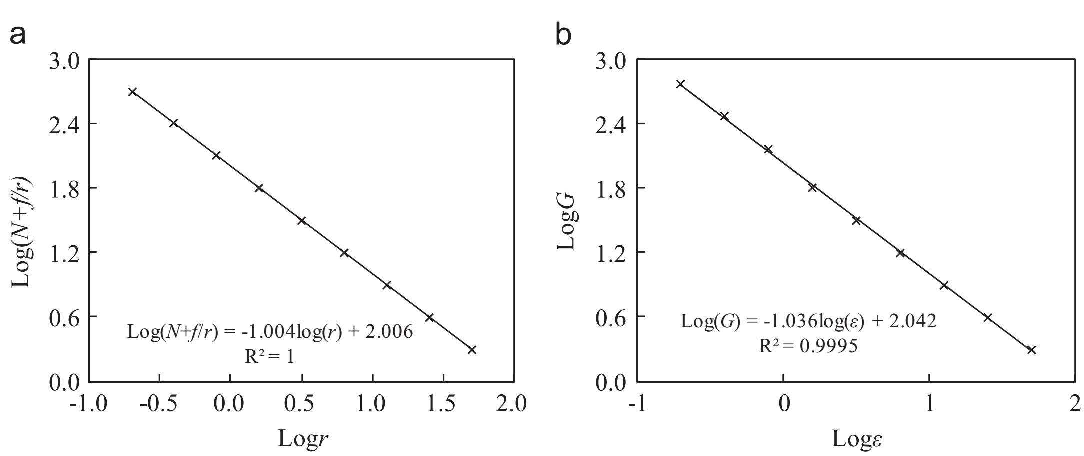

Fig. 4. Scheme of determining *D* by: (a) compass-walking; and (b) box-counting methods (Barton's profile 6–8 as example).

4. Data set

In addition to the 10 standard profiles, this study makes use of another 102 profiles from the literature. Among them, 12 profiles are from Grasselli [38], 26 are from Bandis et al. [39] and the rest (64) are from Bandis [40]. The projected length of the employed 112 profiles ranges from 72 to 119.6 mm, and the *JRC* values range from 0.4 to 20. The rocks these joint profiles come from cover a wide variety of rock types, including sandstone, limestone, marble, granite, gneiss, slate, dolerite and siltstone of various weathering degrees (fresh, slightly weathered and moderately weathered). These joints are tension fractures and vary from well-interlocked planar cleavage fractures to poorly interlocked film-covered walls.

As there were no available digital data of these profiles, the images of these profiles in the original publications in PDF format were imported into AutoCAD. The dimension system of AutoCAD was configured to meet each image by referencing to the scale bar on the original figure. A set of vertical lines spaced 0.4 mm apart were constructed across the length of the profiles. Polylines were used to trace the profiles with the intermediate points falling on the intersection of the vertical lines with the profile. Once each profile was traced, the coordinates defining the polylines were exported to an ASCII file by using a LISP function.

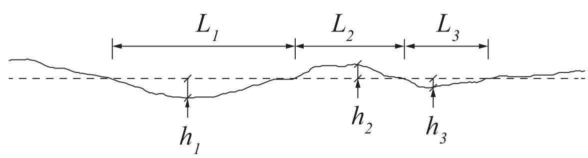

Fig. 5. The updated *h*–*L* method for determining fractal dimension *D*.

It should be noted that some error may be introduced by the above data processing, as this process indeed re-samples the profile which is essentially a re-sampling of the original joint profile. The digitized points of the profiles considered in this study along with the associated back-calculated *JRC* values are supplemented as an electronic resource to this paper. Researchers may make use of them for future investigation without further degradation of the quality of data source.

5. Determination of the fractal dimension, *D*

Following digitization of the profiles, it was found that the best-fit line through all profiles had a non-zero overall slope. To make the profiles horizontally aligned the trend removal was conducted by utilizing a computer program written by the authors.

The other function of this computer program is to perform data validation and determination of fractal dimension for each rock joint profile. For box-counting, the initial length of the box, ε, was set to be half the projected length of the whole profile (as shown in Fig. 4). The second length of the box was half of the first. In this way, the lengths of the box were set as a geometric sequence with a common ratio of 2. The cutoff for the minimum box length was set to be 0.2 mm, which leads to 500 boxes in a row for a 10 cm long profile. The assignment of divider length for compass-walking followed the same method as for box-counting.

After the assignment of the box length and divider length, the program counted the number (*G*) of boxes required to cover the whole profile, the number (*N*) of dividers to walk along the profile

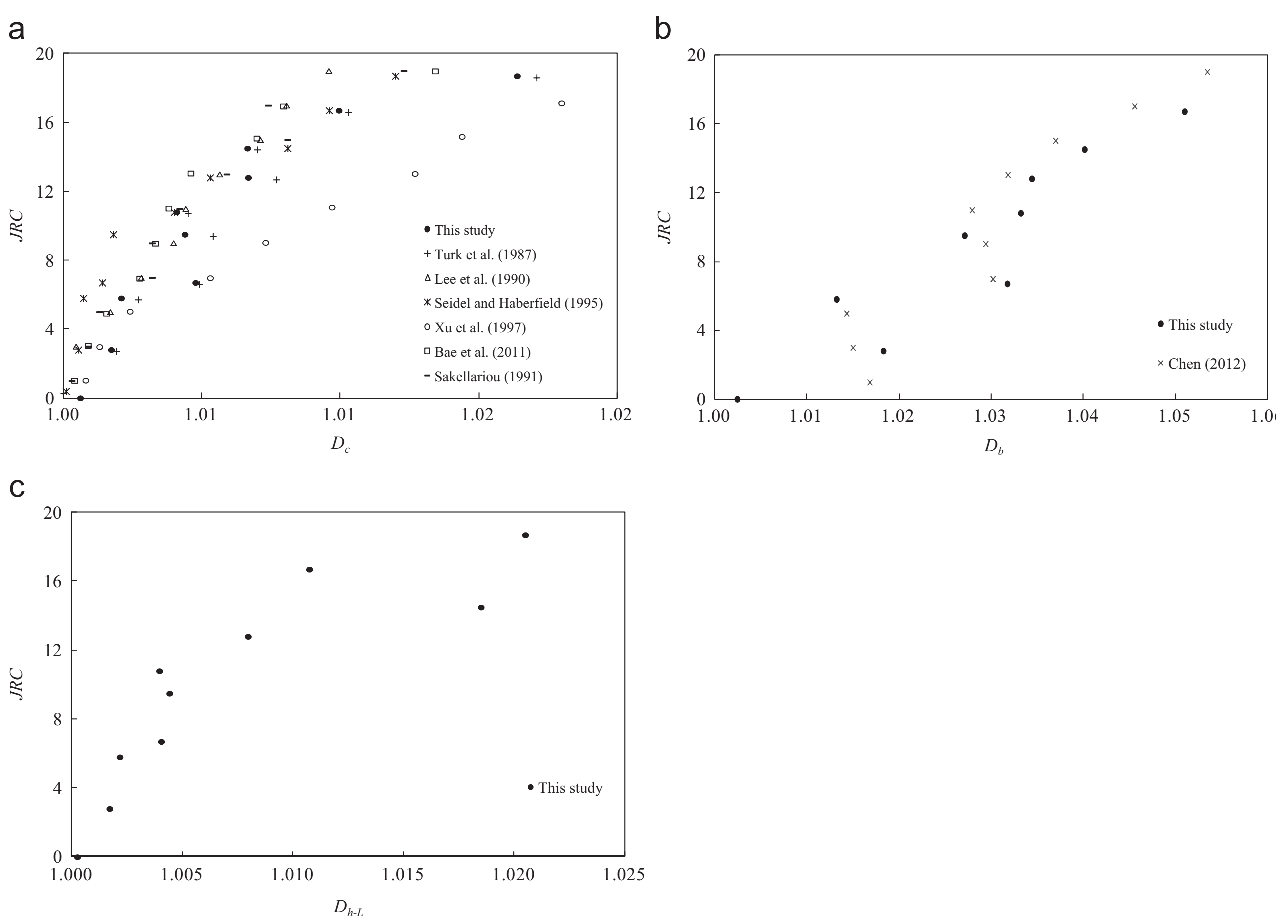

Fig. 6. Fractal dimensions of the 10 standard profiles in the literature and this study by different *D* determination methods: (a) compass-walking; (b) box-counting; and (c) *h*–*L* method.

as well as the remainders (f). The fractal dimension of the examined profile was then obtained by plotting G against ε or $N+(f/r)$ against r in log–log space, as shown in Fig. 4.

As mentioned before, the main difficulty in using the h–L methods proposed by Xie and Pariseau [25] and Askari and Ahmadi [26] is the identification of the "high-order" asperities of a profile (Fig. 2). Accuracy during manually measurement of the base length and height of the identified asperities is another difficulty. An improvement was made in this study (Fig. 5) and the process is as follows: construct the least-square line (dashed line in Fig. 5) on the trend-removed profile; segment the profile by the intersection points; and measure the base length (L) and the extreme peak or valley (h) for each segment. One of the main advantages of this proposal is that it avoids arbitrary identification of "high-order" asperities. This scheme can be performed by a computer program without any subjectivity. The averages of h and

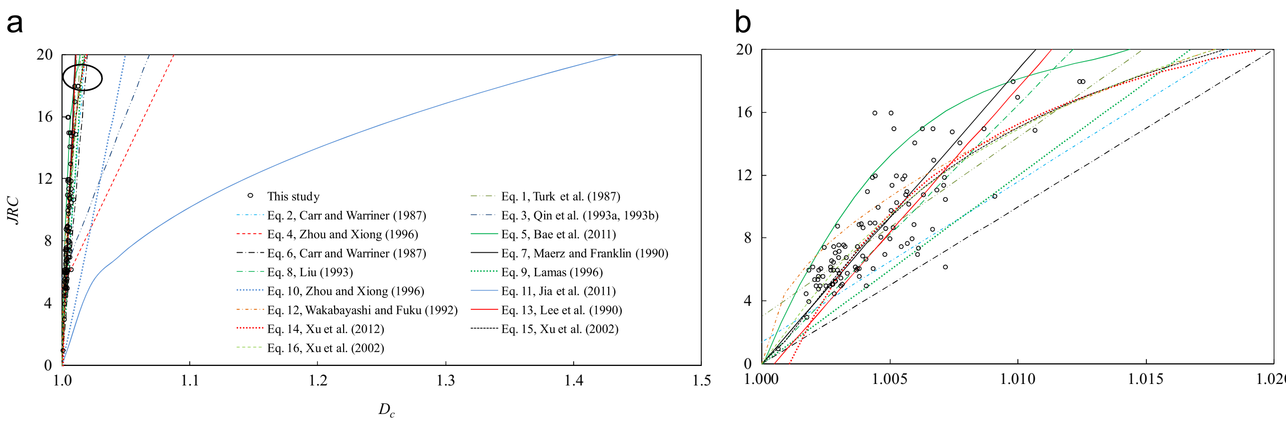

Fig. 7. Verification of correlations between D and JRC in the literature : (a) compass-walking method; and (b) enlargement of the circled part in (a).

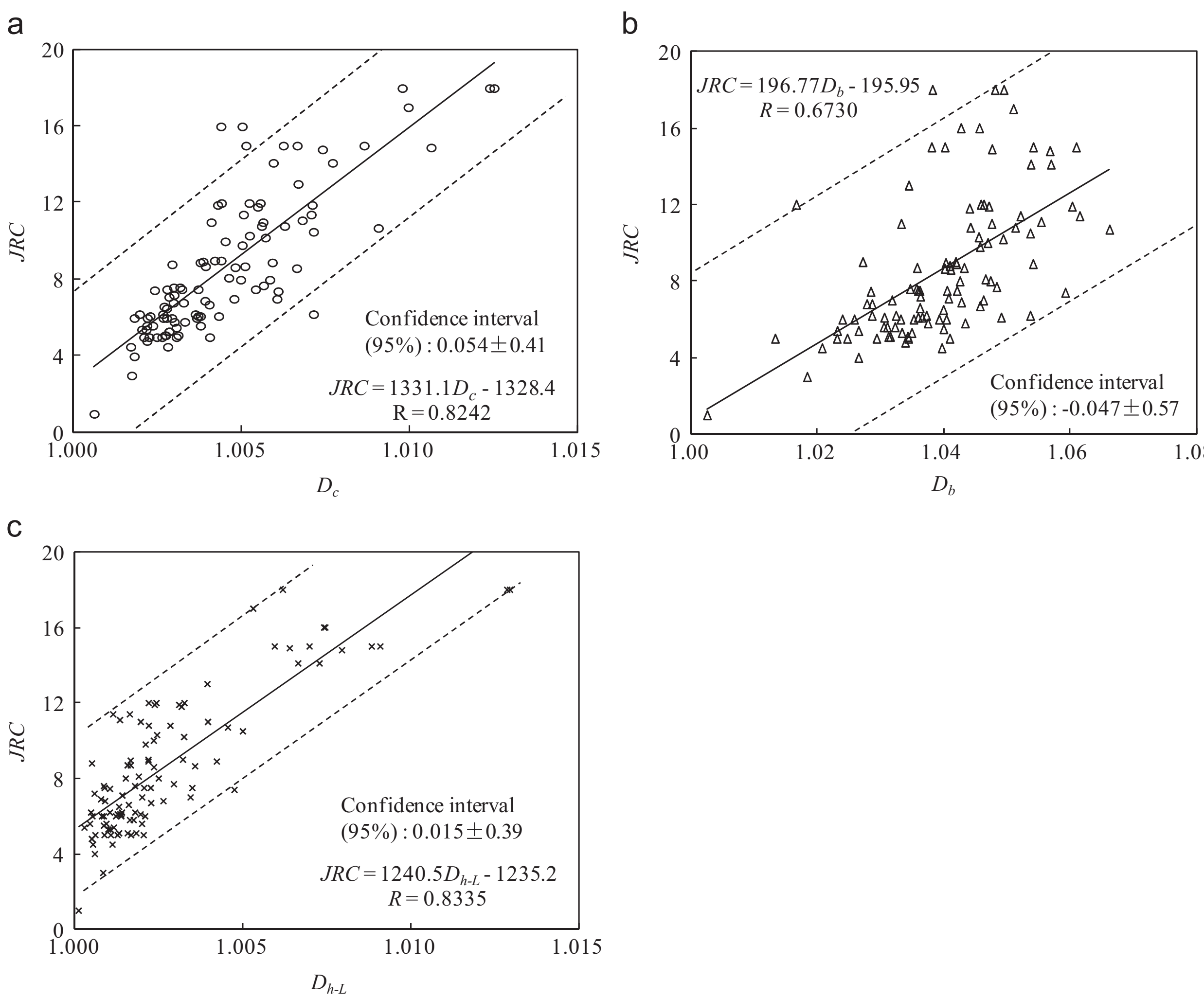

Fig. 8. Relationships between JRC and D in this study: (a) compass-walking; (b) box-counting; and (c) h–L method.

L for a rock joint profile can then be used in the formula of [25] to calculate the fractal dimension.

6. New empirical equations

The data points retrieved from the original figures of the literature are replotted in Fig. 6 together with the D values of this study for Barton's 10 standard profiles. It can be seen that the result of this study is in good agreement with the literature in that JRC increases with D_c, D_b and D_{h-L}. The correlations from the literature and the results of this study are plotted in Fig. 7. Again, equations (T3, T4, T10 and T11) depart far from the main trend of JRC vs. D_c. As the magnified plot (Fig. 7b) shows, equations (T7, T8 and T13) are seemingly consistent with the results of this study. Meanwhile, the remaining equations only appear to be correct over specific ranges of D and JRC. The agreement in Fig. 6 between the literature and this study and the inconsistence in Fig. 7 demonstrate that using only the 10 standard profiles is insufficient for a reliable empirical equation.

The results of D by different methods are plotted in Fig. 8. As indicated, JRC displays a linear relationship with D, although some nonlinear regressions are considered. The 112 data points by compass-walking and h–L method are clustered within a thin band in between the dashed lines. The box-counting method, however, produces a dispersed point set, scattered in a wide area. Thus the relationship between D_b and JRC displays a lower correlation coefficient of about 0.673.

As shown in Fig. 9, JRC also correlates with $D-1$. Table 3 lists the newly developed equations. Power-law equations (E4–E6) are capable of giving a reasonable JRC value to a planar or sub-planar joint profile. Equations (E2) and (E5) are not recommended due to the low correlation coefficients of D_b with JRC. With regard to the usability, equation (E6) may grasp the highest priority due to the easy and convenient determination of D_{h-L}. As its definition in Fig. 5, one can even utilize a spreadsheet to quickly obtain the D_{h-L} by identifying the asperities and obtaining the base length and height of a profile. However, a well-developed computer program may be a need for the determination of D_c. Equations (E1) and (E4) also display good correlation coefficients and are therefore recommended to engineering practice, once a precise D_c can be obtained.

7. Conclusions

This study reviewed estimation of JRC based on the fractal dimension. The methods for determining D and empirical equations relating D to JRC were discussed. Based on the forgoing discussions, the following conclusions can be made.

The fractal dimension can be used to estimate JRC of a rock joint. However, the previous empirical equations show some sizable variations from one another. These variations exist because the data points for deriving these equations are limited and the

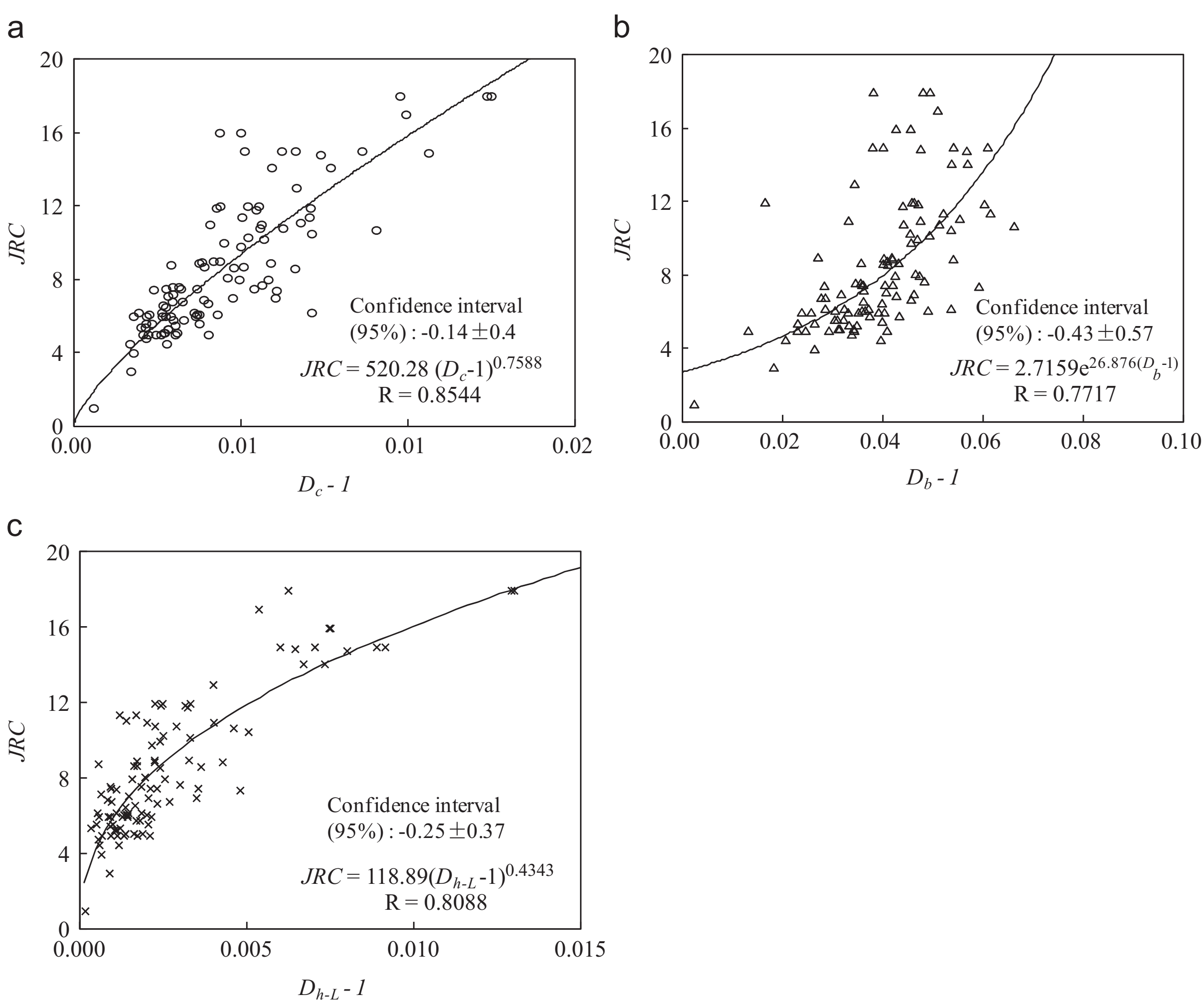

Fig. 9. Relationships between JRC and $D-1$ in this study: (a) compass-walking; (b) box-counting; and (c) h–L method.

Table 3
Equations derived from this study for JRC estimation by using the fractal dimension.

No.	Equation	R	JRC^0	Range[#]
E1	$JRC = 1331.07D_c - 1328.44$	0.8242	2.63	1.0131
E2	$JRC = 196.77D_b - 195.95$	0.6730	0.82	1.0975
E3	$JRC = 1240.46D_{h\text{–}L} - 1235.19$	0.8335	5.27	1.0119
E4	$JRC = 520.28(D_c - 1)^{0.7588}$	0.8544	0	1.0136
E5	$JRC = 2.72e^{26.876(D_b - 1)}$	0.7717	2.72	1.0742
E6	$JRC = 118.89(D_{h\text{–}L} - 1)^{0.4343}$	0.8088	0	1.0165

methods for the determination of D vary. Equations based exclusively on the 10 standard JRC profiles may misestimate the JRC.

This study updated the h–L methods proposed by Xie and Pariseau [25] and Askari and Ahmadi [26]. The updated method can avoid subjectivity during identification of asperities of a joint. The compass-walking, box-counting and updated h–L methods are used in this study to examine 112 joint profiles. It was found that D values determined by the compass-walking and h–L method are more closely related to JRC than those obtained by box-counting. Correlations from this study are considered more reliable due to the large data population and the consistent data processing.

As the employed profiles in this study range from 72 to 119.6 mm in length, which is a narrow band, the authors suggest the equations developed in this study are applicable to laboratory scale. Further study taking profiles of other sizes is demanded. As the sampling interval may influence the correlation between D and JRC, it is suggested to use the equations with a sampling interval of about 0.4 mm. This interval is thought to be easily and conveniently achieved during scanning or digitizing.

It should also be noted that the current study takes 112 rock joint profiles which are currently available in the literature. A bigger sample population would help justify or improve the empirical equations proposed by this study.

Acknowledgments

This study is supported by the National Natural Science Foundation of China (No. 51309176). The authors are grateful to Mr. Mo Ping and Mr. He Shengdi in the laboratory for their help with data preparation.

Appendix A. Supporting information

Supplementary data associated with this article can be found in the online version at http://dx.doi.org/10.1016/j.ijrmms.2015.01.007.

References

[1] Barton N. Review of a new shear-strength criterion for rock joints. Eng Geol 1973;7:287–332.
[2] Barton N, Choubey V. The shear strength of rock joints in theory and practice. Rock Mech 1977;10:1–54.
[3] Brown ET. Rock characterization testing and monitoring (ISRM suggested methods). Oxford: Pergramon Press; 1981.
[4] Tse R, Cruden DM. Estimating joint roughness coefficients. Int J Rock Mech Min Sci Geomech Abstr 1979;16:303–7.
[5] Yu XB, Vayssade B. Joint profiles and their roughness parameters. Int J Rock Mech Min Sci Geomech Abstr 1991;28:333–6.
[6] Yang ZY, Lo SC, Di CC. Reassessing the joint roughness coefficient (JRC) estimation using Z_2. Rock Mech Rock Eng 2001;34:243–51.
[7] Maerz NH, Franklin JA, Bennett CP. Joint roughness measurement using shadow profilometry. Int J Rock Mech Min Sci Geomech Abstr 1990;27: 329–43.
[8] Tatone B, Grasselli G. A new 2D discontinuity roughness parameter and its correlation with JRC. Int J Rock Mech Min Sci 2010;47:1391–400.
[9] Li YR, Zhang YB. Quantitative estimation of rock joint roughness coefficient using statistical parameters. Int J Rock Mech Min Sci. (Under revision).
[10] Turk N, Greig MJ, Dearman WR, Amin FF. Characterization of joint surfaces by fractal dimension. In: Proceedings of the 28th US rock mechanics symposium. Tucson; 1987. p. 1223–36.
[11] Carr JR, Warriner JB. Rock mass classification of joint roughness coefficient. In: Proceedings of the 28th US rock mechanics symposium. Tucson; 1987. p. 72–86.
[12] Mandelbrot BB. Self-affine fractal and fractal dimension. Phys Scr 1985;32: 257–60.
[13] Kulatilake P, Balasingam P, Park J, Morgan R. Natural rock joint roughness quantification through fractal techniques. Geotech Geol Eng 2006;24: 1181–201.
[14] Miller SM,et al. Ambiguities in estimating fractal dimensions of rock fractal surfaces. In: Proceedings of the 31st US Rock Mechanics Symposium. Rotterdam: Balkema; 1990. p. 471–478.
[15] Huang SL, Oelfke SM, Speck RC. Applicability of fractal characterization and modelling to rock joint profiles. Int J Rock Mech Min Sci 1992;29:135–53.
[16] Kulatilake P, Um J, Pan G. Requirements for accurate estimation of fractal parameters for self-affine roughness profiles using the line scaling method. Int J Rock Mech Min Sci 1997;30(4):181–206.
[17] Kulatilake P, Um J, Pan G. Requirements for accurate quantification of fractal parameters for self-affine roughness using the variogram method. Int J Rock Mech Min Sci 1998;35(4):4167–89.
[18] Kulatilake P, Um J. Requirements for accurate quantification of self-affine roughness using the roughness-length method. Int J Rock Mech Min 1999;36:5–18.
[19] Mandelbrot BB. Fractals: form, chance and dimension. San Francisco: WH Freeman; 1997.
[20] Mandelbrot BB. The fractal geometry of nature. San Francisco: WH Freeman; 1983.
[21] Bae D, Kim K, Koh Y, Kim J. Characterization of joint roughness in granite by applying the scan circle technique to images from a borehole televiewer. Rock Mech Rock Eng 2011;44:497–504.
[22] Xu HF, Zhao PS, Li CF, Tong Q. Predicting joint roughness coefficients using fractal dimension of rock joint profiles. Appl Mech Mater 2012;170–173:443–8.
[23] Lee YH, Carr JR, Bars DJ, Hass CJ. The fractal dimension as a measure of the roughness of rock discontinuity profiles. Int J Rock Mech Min Sci 1990;27 (6):453–64.
[24] Cheng Q. Multifractal modeling and lacunarity analysis. Math Geol 1997;29 (7):919–32.
[25] Xie HP, Pariseau WG. Fractal estimation of rock joint roughness coefficient. Sci China 1994;24(5):524–30.
[26] Askari M, Ahmadi M. Failure process after peak strength of artificial joints by fractal dimension. Geotech Geol Eng 2007;25:631–7.
[27] Qin SQ, Zhang ZY, Wang ST, Huang RQ. Fractal features of jointed rock masses and engineering geological significance. J Eng Geol 1993;1(2):14–23.
[28] Jia HQ. Experimental research on joint surface state and the characteristics of shear failure. ([MSc thesis]). Central South University; 2011. p. 86.
[29] Zhou CB, Xiong WL. Relation between joint roughness coefficient and fractal dimension. J Wuhan Univ Hydraul Elect Eng 1996;29(5):1195–7.
[30] Maerz NH, Franklin JA. Roughness scale effect and fractal dimension. In: Rock Masses, Pinto Da Chuha A, editors Proceedings of the 1st international workshop on scale effects. Rotterdam: Balkema; 1990. 121–125.
[31] Liu SY. Fractional dimension method of JRC measurement. Investig Sci Technol 1993;6:26–9.
[32] Lamas LN. An experimental and analytical study of the roughness of granite joints. In: Proc of the Eurock'96, Barla G,.editor. Rotterdam: Balkema; 1996. p. 117.
[33] Wakabayashi N, Fukushige I. Experimental study on the relation between fractal dimension and shear strength. In: Proceedings of the international symposium for fractured and joint rock masses. Berkeley: California; 1992. p. 101–10.
[34] Xu HF, Li YR, Liu XY. Fractal simulation of joint profiles and relationship between JRC and fractal dimension. Chin J Rock Mech Eng 2002;21 (11):1663–6 (In Chinese).
[35] Chen SJ, Zhu WC, Zhang MS, Yu QL. Fractal description of rock joints based on digital image processing technique. Chin J Geotech Eng 2012;34(11):2087–92.
[36] Qin SQ, Zhang ZY, Wang ST, Huang RQ. Fractal features of jointed rock masses. J Chengdu Coll Geol 1993;20(4):109–13.
[37] Seidel JP, Haberfield CM. The application of energy to the determination of the sliding resistance of rock joints. Rock Mech Rock Eng 1995;24(4):211–26.
[38] Grasselli G. Shear strength of rock joints based on quantified surface description. ([Ph.D. thesis]). Ecole Polytechnique Federale De Lausanne (EPFL); 2001.
[39] Bandis SC, Lumsden AC, Barton N. Fundamentals of rock joint deformation. Int J Rock Mech Min Sci 1983;6:249–68.
[40] Bandis SC. Experimental studies of scale effects on shear strength and deformation of rock joint. ([Ph.D. thesis]). Univ. Leeds; 1980.